CHEMISTRY
A EUROPEAN JOURNAL

DOI: 10.1002/chem.200601291

New Light on an Old Story: Formation of Melam during Thermal Condensation of Melamine

Bettina V. Lotsch and Wolfgang Schnick*[a]

Abstract: We report on the existence and formation of the carbon nitride precursor melam $(H_2N)_2(C_3N_3)NH(C_3N_3)(NH_2)_2$, thereby clarifying one of the last unresolved issues posed by the complex thermal condensation of melamine $C_3N_3(NH_2)_3$. Experimental proof is put forward that melam is a direct condensation product of melamine, but can be detected only in small amounts under special reaction conditions owing to its rapid transformation into melem. The coexistence of melamine and melem during thermal condensation yields two adduct phases with distinct compositions $[C_3N_3(NH_2)_3]_2[C_6N_7(NH_2)_3]$ and $[C_3N_3(NH_2)_3][C_6N_7(NH_2)_3]_2$. They may be considered as co-crystallizates of melamine and melem and can be isolated as intermediates between 590 and 650 K prior to the formation of single-phase melem $C_6N_7(NH_2)_3$. Melam (*C*2/*c*, $a=1811.0(4)$, $b=1086.7(2)$, $c=1398.4(3)$ pm, $\beta=96.31(3)°$, $V=2735.3(9)\times10^6$ pm^3, $T=130$ K) adopts a ditriazinylamine-type structure with a twisted conformation about the bridging NH moiety and transforms into melem around 640 K. Two compounds deriving from melam have been synthesized by solution and solid-state reactions. The salt melamium diperchlorate $C_6N_{11}H_{11}(ClO_4)_2\cdot2H_2O$ (*C*2/*c*, $a=1747.8(4)$, $b=1148.2(2)$, $c=993.6(2)$ pm, $\beta=118.79(3)°$, $V=1747.4(6)\times10^6$ pm^3, $T=130$ K) crystallizes as a dihydrate and exhibits a doubly protonated, planar melam core. In the neutral complex $Zn[C_6N_{11}H_9]Cl_2$ ($P2_1/c$, $a=743.00(15)$, $b=2233.2(5)$, $c=762.5(2)$ pm, $\beta=99.86(3)°$, $V=1246.5(4)\times10^6$ pm^3, $T=200$ K), melam acts as a symmetrically bent bidentate ligand, which is coordinated to the Lewis acid Zn-site through two ring nitrogen atoms.

Keywords: carbon nitrides · phase transitions · solid-state structures · thermal decomposition

Introduction

As part of the ongoing quest for graphitic carbon nitride and its potentially ultrahard 3D analogue, the chemical screening of suitable precursors has attracted significant attention in the past few decades. Recently the focus has been shifted to a class of historically important compounds assembled around the common ancestor melamine (triamino-*s*-triazine) $C_3N_3(NH_2)_3$,[1] which constitute the forefront of modern carbon nitride chemistry:[2–21] While the crystal structure of the heptazine derivative melem $C_6N_7(NH_2)_3$ has been elucidated only recently,[22,23] the existence and, above all, molecular structures of the conjectured condensation products of melamine, melam $[(H_2N)_2(C_3N_3)]_2NH$ and melon "$[C_6N_7(NH)(NH_2)]_n$", have not been ultimately clarified due to the lack of crystallographic data.[24,25–29] Owing to their prototypic carbon(IV) nitride backbones, resolving the identities of these potential CN_x precursors may entail far-reaching implications for the structure and formation of g-C_3N_4, at the same time shedding light on the historically as well as industrially important thermolysis reaction of melamine.

Melam was first prepared in 1834 by Liebig on heating an intimate mixture of potassium thiocyanate and an excess of ammonium chloride at temperatures around 580–640 K. From the fusion product a compound was isolated, after treatment with potassium hydroxide solution, which was arbitrarily given the name "melam" by Liebig.[1] Since the 19th century much effort has been devoted to the elucidation of the composition and structure of the pyrolysis products of melamine, which, however, was hampered by conflicting statements with respect to their elemental composition and ways of formation.[24,25,30,31] Whereas the identity of melamine was resolved by the elucidation of its crystal

[a] Dr. B. V. Lotsch, Prof. Dr. W. Schnick
Department Chemie und Biochemie, Ludwig-Maximilians-Universität, Butenandtstraße 5–13 (D), 81377 München (Germany)
Fax: (+49) 89-2180-77440
E-mail: wolfgang.schnick@uni-muenchen.de

Supporting information for this article is available on the WWW under http://www.chemeurj.org/ or from the author.

structure in 1941,[32] chemical inertness and low solubility of its condensation products has impeded thorough characterization ever since their early discovery.

Melam has been considered the low-temperature de-ammonation product of melamine, which is formed upon linking two molecules of melamine with concomitant release of one mole of ammonia. The resulting "ditriazinylamine"-type structure model was set out as early as 1886 by Klason[33] and accepted by later investigators.[24,25,34,35] Doubts about the correctness of this proposed structure arose following several unsuccessful attempts to obtain melam by pyrolyzing melamine, the products of which were identified as melem by IR and UV spectroscopy.[27–29,36,37] In contrast, May reported on the isolation of melam, melem, and melon as the pyrolysis products of melamine obtained at 633, 673, and 773 K, respectively, based on elemental analysis.[26] The two alternative schemes proposed in the literature for the condensation process of melamine are outlined in Scheme 1.

Route **a** is based on the formation of melem as the first condensation product, giving rise to a ratio of melamine to liberated ammonia of 1:1. Melem then affords the polymeric condensate melon, the identity of which has not been resolved as yet.[27,29,37] Melon may further lose ammonia to form graphitic carbon nitride g-C_3N_4, which, however, has not been proven until know and is subject of ongoing speculation. In Route **b**, melamine progressively condenses to graphitic carbon nitride via melam (melamine/ammonia = 2:1), melem, and melon (Scheme 1).[26,38,39] A detailed understanding of the pyrolysis of melamine, however, seems to be pivotal to clarify the stability ranges of triazine and heptazine systems with respect to the structure elucidation of g-C_3N_4.[2–4,13,28,29]

While the originally proposed formula for melam as sketched in Scheme 1 has long been acknowledged, an alternative tautomeric form was introduced, accounting for resonance within the two triazine rings (Scheme 2).[27,39,40]

Despite the above controversy, reports have been published on the synthesis of melam and substituted melams

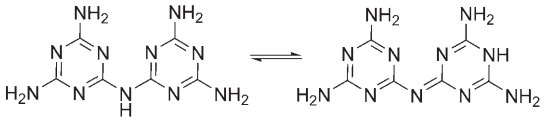

Scheme 2. Two alternative tautomeric forms discussed for melam. The conjugated form (right) exhibits a quinoid triazine ring system.

based on combinations of (alkyl-substituted) aminotriazines with electrophilic triazine derivatives such as chlorotriazines.[40,41] The chloro derivatives of melam $HN(C_3N_3Cl_2)_2$ and $N(C_3N_3Cl_2)_3$ were recently obtained by the reaction of melamine with cyanuric chloride and are being discussed as potential intermediates in the formation of polymeric C_3N_4 compounds.[15,42] Presently, melam and its derivatives are under consideration as flame-retardant formulations owing to their exceptional thermal stability and decomposition properties.[43–45] The synthesis of melam salts from melamine in the presence of acids, among which is a zinc salt of assumed formula $Zn^{2+}[C_6N_{11}H_8]^-_2$, has been reported; however, no analytical data except for elemental analysis in the latter case are available.[28,46] Costa and Jürgens have investigated the thermal behavior of melamine salts, thereby coming across melam hydrohalides and their ammonium chloride adducts of the empirical compositions $C_6N_{11}H_9{\cdot}HBr$ and $[C_6N_{11}H_{10}]X{\cdot}0.5\,NH_4X$ (X = Cl, Br), whose structures could, however, not be elucidated.[47,48]

According to the literature data summarized above, the knowledge on the formation of melam from melamine, as well as its molecular structure, is scarce and subject to much controversy. In the following we will comprehensively sketch the thermal behavior of melamine and present an alternative view on the formation and existence of melam.

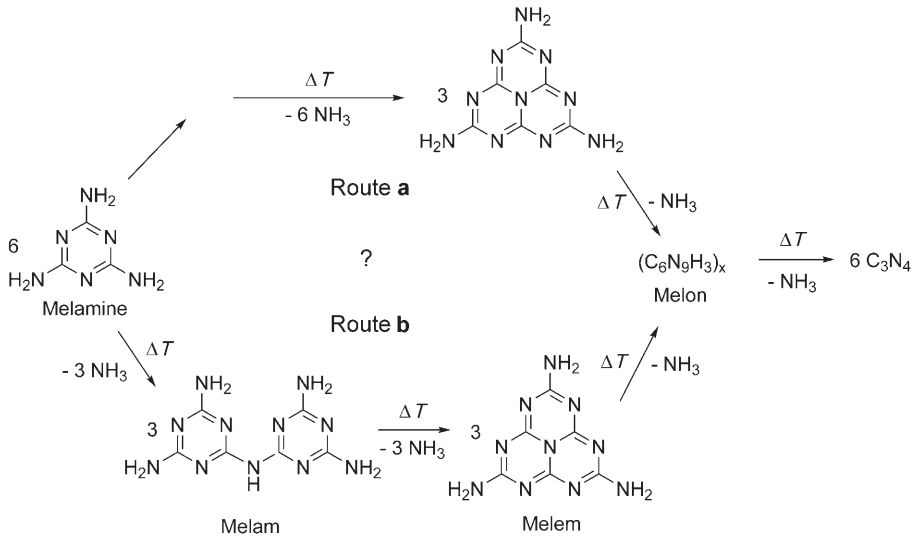

Scheme 1. Schematic representation of the two pathways proposed for the thermal decomposition of melamine. Route **a** assumes direct formation of melem in the first condensation step, whereas according to Route **b** melam is obtained prior to melem formation. Further loss of ammonia may yield polymers of melem ("melon") and, ultimately, graphitic carbon nitride.

Results and Discussion

Thermal behavior of melamine: A crucial factor when investigating the thermal behavior of melamine is the choice of the reaction conditions. Typically, such studies have been conducted in closed systems, as melamine exhibits a strong tendency toward sublimation above 570 K, which peaks around 618 K. A lack of clarity,

however, remains with regard to the processes taking place in this temperature range, as it has not yet been specified whether or to what extent melamine undergoes sublimation,[29] melting,[27,36] or condensation reactions.

We have performed temperature-programmed XRD measurements (TPXRD) with heating rates of 1 K min^{-1} in a temperature range between 298 and 933 K (Figure 1). It

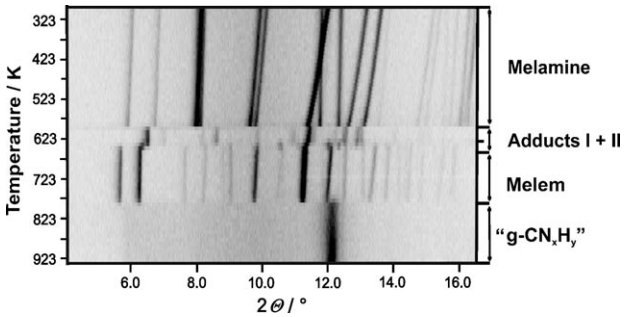

Figure 1. In situ temperature-programmed X-ray powder diffraction measurements ($Mo_{K\alpha1}$ radiation) of melamine recorded between room temperature and 923 K. Four phase transitions are observed prior to the formation of a graphitic carbon nitride material visible by a broad reflection at $2\theta \approx 12.1°$ ($d \approx 336$ pm).

should be noted that heating a sample in an open quartz capillary affords conditions similar to those in closed systems as has been observed previously.[20] We will therefore use the term "semi-closed system" for this experimental set-up.

Under the slow heating conditions applied, at least four transformations are observed: The reflections of melamine disappear at 590 K without passing through an amorphous state, with the new phase being stable up to approximately 630 K. At this temperature, new reflections gradually appear, the phase change being defined rather poorly. Melem is formed around 653 K and is stable up to 780 K, at which temperature a single broad reflection characteristic of so-called graphitic carbon nitride materials emerges, again without passing through the melt.

When comparing with the above literature survey (cf. Scheme 1), Route b conforms quite well to these observations, whereas the direct formation of melem from melamine (Route a) without the formation of intermediates detectable by in situ X-ray diffraction can be discarded under these conditions. The observed low-temperature (LT) phase transition may tentatively be associated with the proposed formation of melam, which, however, does not account for the second phase change (HT phase transition) observed at 630 K prior to the formation of melem.

Upon trying to isolate the above phases ex situ, a strong dependence on both temperature *and* time is perceivable, as the HT phase (phase II) is formed by isothermal treatment from the low-temperature phase (phase I), the same applying to the formation of melem from the high-temperature phase. After optimizing the heating conditions, both phases could be isolated in a pure state without admixtures of melamine, melem, or phases I/II detectable by X-ray diffraction as shown in Figure 2. All efforts to index the powder diffractograms or grow single crystals were unsuccessful. Consequently, the characterization of the two phases was conducted by spectroscopic methods.

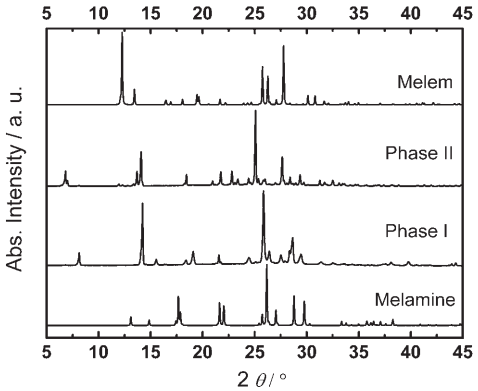

Figure 2. X-ray powder patterns ($Cu_{K\alpha1}$ radiation) of melamine, phase I, phase II, and melem (bottom to top) recorded at room temperature. All compounds exhibit well distinguishable powder patterns indicative of distinct crystallographic phases.

Adduct phases: Mass spectrometry was carried out as a first step to identify the intermediate LT and HT phases. For both phases, only peaks at *m*/*z* 126 and 218 were detected, which correspond exactly to the molecular mass peaks of melamine and melem, respectively. At the same time, no evidence was found for melam at *m*/*z* 235. According to these results, which conform to the observations previously made by Jürgens,[48] strong evidence is put forward for melamine and melem instead of melam to actually constitute the phases under consideration.

The composition of both phases was determined by elemental analysis; the results are listed in Table 1. It is evident that the composition of phase I indeed closely corresponds to that of melam as stated by May and others.[26,38,39] The composition of phase II, however, neither matches that of melamine, nor that of melam or melem to a first approxima-

Table 1. Elemental analysis data observed and calculated for different compounds and compositions.

Compound	Sum formula	N [wt %]	C [wt %]	H [wt %]
phase I		65.93 (obs.)	30.56 (obs.)	3.63 (obs.)
phase II		64.73 (obs.)	32.14 (obs.)	3.21 (obs.)
melamine	$[C_3N_6H_6]$	66.67 (theor.)	28.57 (theor.)	4.76 (theor.)
melam	$[C_6N_{11}H_9]$	65.53 (theor.)	30.64 (theor.)	3.83 (theor.)
melem	$[C_6N_{10}H_6]$	64.22 (theor.)	33.03 (theor.)	2.75 (theor.)
2:1 adduct[a]	$[C_3N_6H_6]_2[C_6N_{10}H_6]$	65.53 (theor.)	30.64 (theor.)	3.83 (theor.)
1:2 adduct[b]	$[C_3N_6H_6][C_6N_{10}H_6]_2$	64.77 (theor.)	32.02 (theor.)	3.18 (theor.)

[a] melamine/melem = 2:1. [b] melamine/melem = 1:2.

tion. Anticipating the results discussed below, the following noticeable detail may be pointed out:

In view of the fact that the elemental composition of melam is in between those of melamine and melem, it may be possible to obtain an identical composition by assembling melamine and melem in different ratios into a co-crystal. This has formally been done for two compositions according to a 2:1 adduct of melamine and melem, as well as a 1:2 adduct, the theoretically expected compositions of which are given in Table 1. Interestingly, the 2:1 adduct has exactly the same composition as melam, and is thus in agreement with the experimental data obtained for phase I. With similar precision the compositions of phase II and the 1:2 adduct can be considered identical. These observations thus nicely explain the results from mass spectrometry, which yield only the molecular mass peaks of melamine and melem.

We therefore emphasize that an ultimate proof of melam formation solely based on elemental analysis data is intrinsically critical and requires corroboration by complementary methods. To further substantiate this hypothesis, the results from complementary analytical techniques will be discussed in the following.

The IR spectra of phases I and II are shown in Figure 3 (bottom), together with the spectra of melamine and melem (top) for comparison. The principal absorption "envelopes" of phases I and II in the characteristic ring-stretching and NH_2-bending region of strongest absorption between 1350 and 1700 cm^{-1} are largely identical, apart from pronounced differences of the relative band intensities and splittings. Whereas for phase II (top) a split band is seen at 1600–1630 cm^{-1}, this band is broadened and slightly weaker in the spectrum of phase I (bottom). However, bands at 1585 and 1561 cm^{-1} observed for the latter, which are typical of triazine-based compounds, are absent in phase II. Remarkably, whereas for melamine a band assigned to $\delta(NH_2)$ is visible at 1650 cm^{-1}, no absorption is found for both I and II higher than about 1630 cm^{-1}, which may be indicative of a significantly altered hydrogen-bonding network. This is supported by the fact that the sharp ν(NH) stretching vibrations for melamine at 3468 and 3419 cm^{-1} are replaced by a weak, though sharp band centered at about 3464 cm^{-1} for I and II. Phases I and II exhibit a strong *split* band around 800 cm^{-1} attributable to the sextant bend of both triazine and heptazine rings, which is located intermediate between those found in melamine and melem, respectively. Although no ultimate conclusions can be drawn from vibrational spectroscopy, the following aspects may be pointed out:

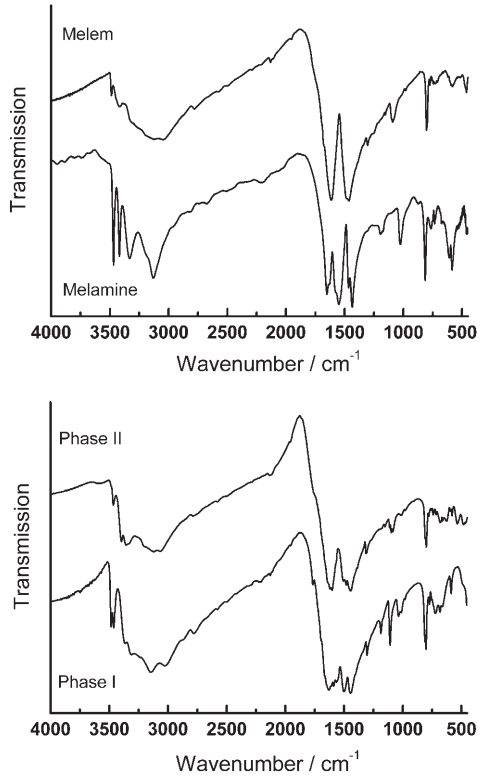

Figure 3. Top: FTIR spectra of melamine (bottom curve) and melem (top curve). Bottom: FTIR spectra of the LT phase I (bottom curve) and the HT phase II (top curve), measured as KBr pellets.

For melam one would expect more pronounced absorption in the ν(C–N) region between 1200 and 1350 cm^{-1} (see below), which is not observed for I and II. A simple superposition of the spectra of melamine and melem can also be discarded (see also XRD results, Figure 2), as too many band shifts are observed for both phases relative to the former. Nevertheless, a particularly significant similarity between the spectrum of phase II and that of melem is evident. In addition, the overall resemblance of the spectra for I and II suggests that the two phases are related with respect to their constituents.

NMR investigations have been carried out both in the solid state and in solution. The ^{15}N solid-state NMR experiments greatly suffer from the long relaxation times of the samples, rendering the signal-to-noise ratio rather low. The ^{13}C CP-MAS solid-state NMR spectrum of phase I shows two signal groups, of which one is located at $\delta = 155.3$ ppm, and a split signal has maxima at $\delta = 166$ and 168 ppm (Figure 4, top). A similar spectrum, yet with a slight high-field shift of the signal group now centered around $\delta =$ 166 ppm, is obtained for phase II (Figure 5, top). While the resonance at $\delta = 155.3$ ppm is unchanged, the intensity at $\delta = 165.0$ ppm is increased, and the signal portion around $\delta = 167.4$ ppm is reduced with respect to phase I. Both "patterns" contain features reminiscent of melem (middle curve),[22,48] whose peaks are located at $\delta = 155.1/156.0$ ppm and $\delta = 164.3$–166.4 ppm, and melamine, which has two close-by signals at $\delta = 167.5$ and 169.2 ppm (bottom curve). Hence, from the ^{13}C spectra of the two intermediates an increasing similarity with melem becomes evident on going from phase I to phase II.

The ^{15}N spectrum of phase I exhibits peaks between $\delta =$ −198 and −210 ppm and two signals in the high-field region ($\delta = -274$ ppm, doublet at $\delta = -291/-294$ ppm, Figure 4, bottom). To assess the ^{15}N proton environment, a CPPI experiment has been carried out (see Figure S1 in the Supporting Information). In agreement with its chemical shift, the

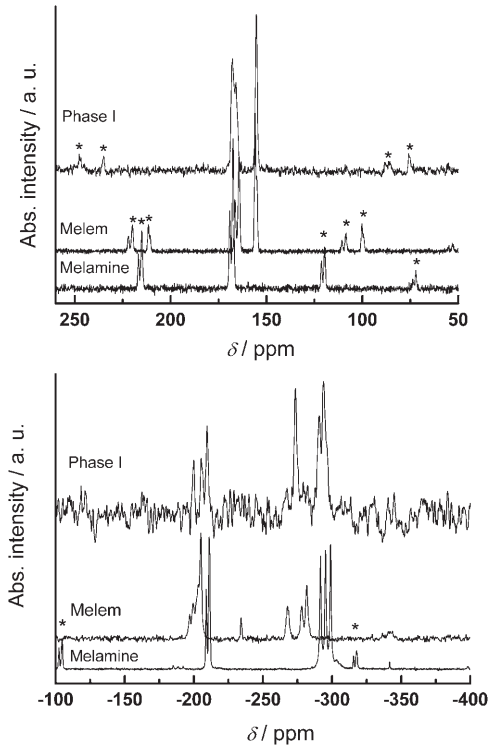

Figure 4. ^{13}C (top) and ^{15}N (bottom) CP-MAS solid-state NMR spectra of the LT phase I (top curve; recycle delay: 300 s; τ_c: 4 ms for both measurements; spinning frequency 10 kHz) in comparison with melem (middle curve; recycle delay: 160 (^{13}C) and 30 s (^{15}N); τ_c: 4 ms for both measurements; spinning frequency: 7 kHz) and melamine (bottom curve; recycle delay: 20 s; τ_c: 8 ms (^{13}C) and 4 ms (^{15}N); spinning frequencies: 6 kHz (^{13}C) and 5.5 kHz (^{15}N). The signal assignments for phase I were additionally corroborated by means of a CPPI experiment (see text). Spinning side bands are marked by asterisks.

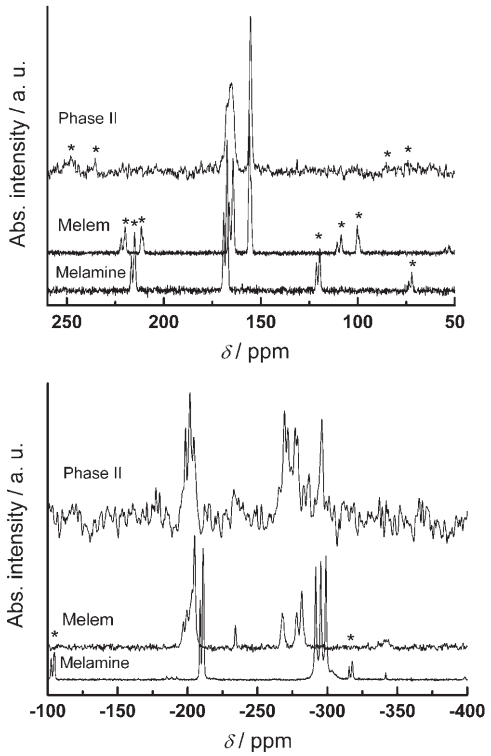

Figure 5. ^{13}C (top) and ^{15}N (bottom) CP-MAS solid-state NMR spectra of the HT phase II (top curve; recycle delay: 360 s; τ_c: 4 ms for both measurements; spinning frequency 10 kHz) in comparison with melem (middle curve) and melamine (bottom curve, for parameters cf. Figure 4). Spinning side bands are marked by asterisks.

signal group centered at $\delta = -200$ ppm can be assigned to tertiary nitrogen atoms, whereas the signals below $\delta = -270$ ppm were identified as NH_2 groups owing to their characteristic polarization inversion behavior.[21,22,48,49] The nitrogen resonance expected for the central ^{15}N nucleus of the heptazine core is not observed in the experiment, which may be a natural consequence of the low signal-to-noise ratio.

The ^{15}N spectrum of phase II exhibits both slightly different signal positions and numbers, with an increase of signal multiplicity in the chemical shift region characteristic of the melem-type N_{tert} and NH_2 groups ($\delta = -198.5$ to -204.4 ppm and $\delta = -269.2$ to -295.9 ppm). Remarkably, the two upfield NH_2 signals in phase I, which may be attributable to the triazine part of the compound, are collapsed to one single resonance at $\delta = -295.9$ ppm in phase II. The signals of the presumed triazine nitrogen atoms typically observed around $\delta = -210$ ppm in melamine and phase I is obviously shifted down-field in phase II (Figure 5, bottom). A resonance attributable to the central nitrogen atom of the cyameluric nucleus can be weakly distinguished at $\delta = -233$ ppm. The following aspects need to be emphasized:

Although the spectra of phases I and II largely parallel those of melamine and melem with respect to the signal positions, obvious differences are observed regarding the number of signals, especially if the NH_2 regions for phases I and II are compared to those of melem and melamine, respectively. This observation may reflect the varying ratios of melamine and melem in the two adduct compounds, as well as pronounced differences in terms of the molecular arrangements in the solid state.

Notably, the lack of signals pertaining to NH groups is a strong indication that none of the nitrogen atoms of the constituents of phases I and II is protonated (or deprotonated), and that no larger molecular aggregates condensed via NH bridges are present. This, however, further substantiates the view that both phases are built up by a co-crystallizate of melamine and melem, forming an array glued together by hydrogen-bonding forces rather than by acid–base or cross-linking reactions. The noticeable differences between the spectrum of phases I and II on the one hand, and that of a simple superposition of the spectra of melamine and melem on the other hand, suggest that no simple heterogeneous mixture of melamine and melem crystals is present, and that the molecular arrangement and intermolecular forces in the adduct phases are significantly different from those dominant in the crystal structures of the pure compounds.

Figure 6 outlines the solution NMR spectra of adducts I and II, as well as those of melamine and melem for comparison. Most notably, this time the spectra of I and II appear to be identical to a superposition of those of melamine and melem, the chemical shift of both ^{1}H and ^{13}C signals being largely identical.[50]

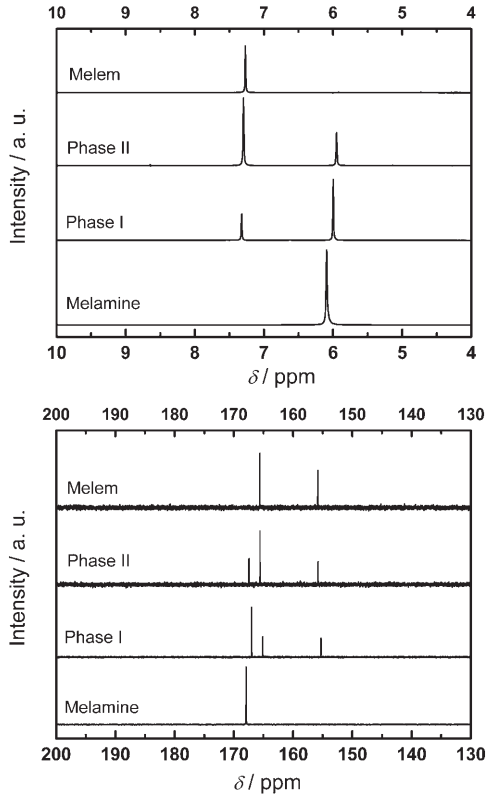

Figure 6. ^{1}H (top) and ^{13}C (bottom) NMR spectra of adducts I and II measured in [D_6]DMSO solution. The respective spectra of melamine (bottom) and melem (top) are shown for comparison.

Whereas for phase I, the intensity of the proton signals belonging to melamine outweighs that of the melem protons (ratio $\approx$2.3:1.0), the situation is opposite for phase II (ratio $\approx$1.4:2.0). These findings must, however, be treated with some caution, as in both cases the sample was not completely dissolved in DMSO, so that a preferential uptake of a single component may not be excluded. Nevertheless, the significant variation in the intensities between phase I and II, together with the results from elemental analysis, suggest that the latter effect may not be particularly strong and the general trend can nevertheless be derived.

Chemical evidence for the disintegration of the adduct phases in solution was obtained by boiling a suspension of I and II, respectively, in water so as to "extract" melamine, which is soluble in hot aqueous solution. In fact, melamine was isolated from the filtrates, whereas the white residues of adduct I and II exhibit identical IR spectra, which were identified as melem–hydrate phases (see Figure S3 in the Supporting Information).

These results corroborate the above line of argument that phases I and II in fact consist of co-crystals formed by melamine and melem in two different, yet well-defined ratios.

Although no evidence for melam was found by thermal decomposition of melamine under the above conditions, the existence of melam cannot be disputed based on these findings alone. It may not even be legitimate to reject the possibility that melam is indeed formed as a condensation product of melamine if different reaction conditions apply. To pursue this thread, the decomposition of melamine under atmospheric pressure was studied.

Melam: When melamine was pyrolyzed in a porcelain crucible only loosely covered with a lid and placed in a muffle furnace at 613–633 K for approximately two days, tiny colorless crystals formed on the surface of the grayish bulk material. These crystals, which may easily be taken for melamine, were identified as melam (**1**) by single-crystal X-ray analysis.[51] The X-ray powder pattern of the bulk material resembles that of a mixture of impure adduct phases I and II, though of poor crystallinity. Melam is either formed as a minor side product, or most likely further transformed into melem with a high rate constant, such that it is essentially invisible in the in situ X-ray powder patterns. In accord with the latter conjecture, all melam crystals completely vanish on prolonged heating at the same temperature.

Although based on this observation the existence of melam has been unambiguously proven, we note that it is detectable only if the heating and tempering conditions are very carefully chosen. It appears that only a certain time-window, as well as the condition of atmospheric pressure, allow the observation of melam.

Melam crystallizes in the space group *C*2/*c* with 1.5 formula units in the monoclinic unit cell, such that two crystallographically independent melam molecules are present. Relevant crystallographic data are given in Table 2. The molecular structure is characterized by two triazine units condensed through a bridging NH group (Figure 7). As melam is non-protonated, both rings are essentially equivalent which is in agreement with the special position occupied by N15 and the generation of the second triazine unit by symmetry. Although the second melam molecule is fully contained in the asymmetric unit, both triazine rings exhibit similar features and are grouped around N4 in a "staggered" arrangement. It should be noted at this stage that the hydrogen positions at the bridging nitrogen atoms have been found explicitly from difference Fourier syntheses, therefore supporting the tautomeric form without conjugation between the triazine ring systems ("ditriazinylamine", see Scheme 2, left).

Notably, the melam molecules are not planar but are twisted about the central nitrogen atom, and display dihedral angles about the bridging NH groups of about 11° (N15) and 14° (N4), respectively. Accordingly, the amino groups attached to the triazine rings do not interfere, which together with a more efficient hydrogen bonding network may be the reason for the observed nonplanarity. The angle

Table 2. Selected crystallographic data for melam (**1**), melamium perchlorate hydrate (**2**), and the Zn–melam complex (**3**).

	1	**2**	**3**
empirical formula	$C_6N_{11}H_9$	"$[C_6N_{11}H_{11}]\cdot 2\,ClO_4\cdot 2\,H_2O$"[a]	$Zn[C_6N_{11}H_9]Cl_2$
molar mass [g mol^{-1}]	235.24	472.84	371.51
crystal system	monoclinic	monoclinic	monoclinic
space group	*C*2/*c* (no. 15)	*C*2/*c* (no. 15)	$P2_1/c$ (no. 14)
temperature [K]	130	130	200
diffractometer, monochromator	Enraf–Nonius Kappa CCD, graphite	STOE IPDS, graphite	Enraf–Nonius Kappa CCD, graphite
radiation, λ [pm]	$Mo_{K\alpha}$, 71.073	$Mo_{K\alpha}$, 71.073	$Mo_{K\alpha}$, 71.073
Z	12	4	4
unit cell dimensions			
a [pm]	1811.0(4)	1747.8(4)	743.0(2)
b [pm]	1086.7(2)	1148.2(2)	2233.2(5)
c [pm]	1398.4(3)	993.6(2)	762.5(2)
β [°]	96.31(3)	118.79(3)	99.86(3)
volume [10^6 pm^3]	2735.3(9)	1747.4(6)	1246.5(4)
calculated density [g cm^{-3}]	1.714	1.797	1.980
crystal size [mm^3]	$0.20\times0.12\times0.04$	$0.23\times0.14\times0.12$	$0.16\times0.12\times0.03$
absorption coefficient [mm^{-1}]	0.127	0.453	2.409
diffraction range [°]	$3.56\le\theta\le27.48$	$3.66\le\theta\le27.49$	$3.27\le\theta\le27.50$
index range	$-23\le h\le23$	$-22\le h\le22$	$-9\le h\le9$
	$-13\le k\le14$	$-14\le k\le13$	$-28\le k\le29$
	$-18\le l\le18$	$-11\le l\le12$	$-9\le l\le9$
parameters/restraints	285/0	170/0	217/0
total no. reflections	5976	7067	5595
independent reflections	3125 ($R_{int}=0.0162$)	1907 ($R_{int}=0.0359$)	2857 ($R_{int}=0.0378$)
observed reflections	2706	1620	2186
GooF on F^2	1.048	1.058	1.057
final *R* indices [$I>2\sigma(I)$]			
(all data)			
*R*1	0.0350 (0.0414)	0.0400 (0.0493)	0.0306 (0.0505)
*wR*2	0.0926 (0.0970)	0.1009 (0.1048)	0.0697 (0.0754)
min./max. residual electron density (e$\times10^{-6}$ pm^{-3})	−0.244/0.205	−0.437/0.465	−0.491/0.345

[a] Idealized formula.

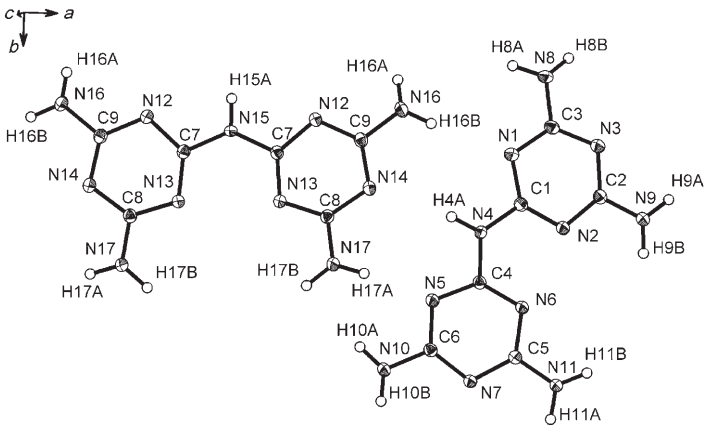

Figure 7. Representation of the molecular structure of melam. The two crystallographically independent melam molecules are shown. Thermal displacement ellipsoids (except for H) are drawn at the 50% probability level.

C-N-C at the NH group is significantly widened (129° (N4), 132° (N15)) and strongly deviates from tetrahedral symmetry, giving rise to a rather trigonal-planar arrangement. The C–NH–C bond lengths are up to 4 pm longer than those in the triazine rings (see below). The amino groups also depart from planarity in that they slightly bend out of the triazine ring plane. This may be indicative of only moderate participation of the free electron pair at the amino nitrogen atoms in the ring π system, which is supported by the fact that the C–N_{ext} bonds (133–135 pm) are slightly elongated by analogy with melamine.[32] Another feature is the obvious distortion of the triazine rings, which are neither completely flat nor regular hexagons, the latter being characteristic of triazine rings: While the N-C-N angles are close to 126°, the C-N-C angles vary between 113° and 114°. The C–N bond lengths within the rings do not vary to a large extent, amounting to 134–135 pm on average, whereas the bonds C4–N6, C1–N2, and C7–N13 adjacent to the bridging NH group are systematically shorter (133 pm).

The molecules are connected through medium strong and weak hydrogen bonds with donor–acceptor distances ranging from 297 to 333 pm. No pronounced π-stacking is observed, reflected by a screwlike arrangement of the molecules, which gives rise to a 3D network of mutually tilted melam molecules (Figure 8).

The IR spectrum of melam is displayed in Figure 9. The similarities to the spectrum of melamine (Figure 3, top) is evident, which is particularly pronounced in the ν(NH) region above 3100 cm^{-1} as well as for the $\delta(NH_2)$ and ν(C=

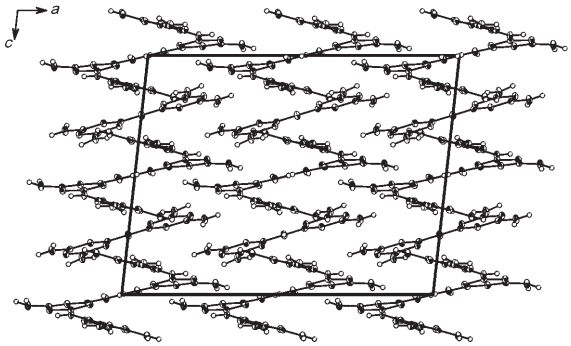

Figure 8. Unit cell of melam (view along [010]), showing the spatially extended, spiral-type stacking of the molecules. Thermal displacement ellipsoids (except for H) are drawn at the 50% probability level.

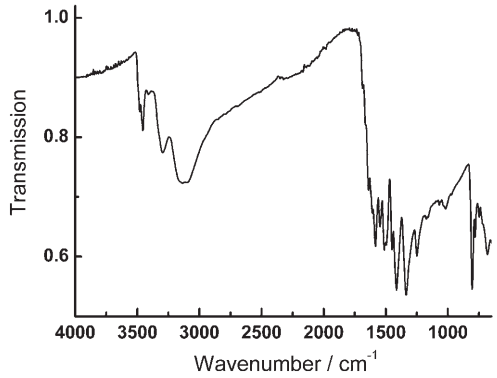

Figure 9. FTIR spectrum of melam, recorded at room temperature between 4000 and 650 cm^{-1} in reflection geometry (neat solid).

N) absorption between 1640 and 1414 cm^{-1}. Though having similar intensities, the latter bands are well resolved and sharp in contrast to those of melamine, and an additional band at 1583 cm^{-1} is found for melam that is absent in both melamine and melem. Similar to melamine, the characteristic sextant ring bend is located at 807 cm^{-1}. Whereas for melamine and melem no pronounced absorption is found below 1400 cm^{-1}, two strong bands attributable to the ν(C–N) and δ(NH) vibrations are found for melam at 1338 and 1250 cm^{-1}.

^{13}C CP-MAS NMR spectroscopy (Figure 10, top) reveals two close-by signals at $\delta = 164.0$ and 167.2 ppm, the latter having a shoulder on the high-field side. Presumably, these hardly separable resonances correspond to the three distinguishable carbon sites within a single triazine nucleus. The theoretically possible number of nine carbon sites can clearly not be resolved. The chemical shift values are almost identical with those observed for melam hydrate (not shown) and very similar to the signal positions in the $ZnCl_2$–melam complex (see Figure 14).

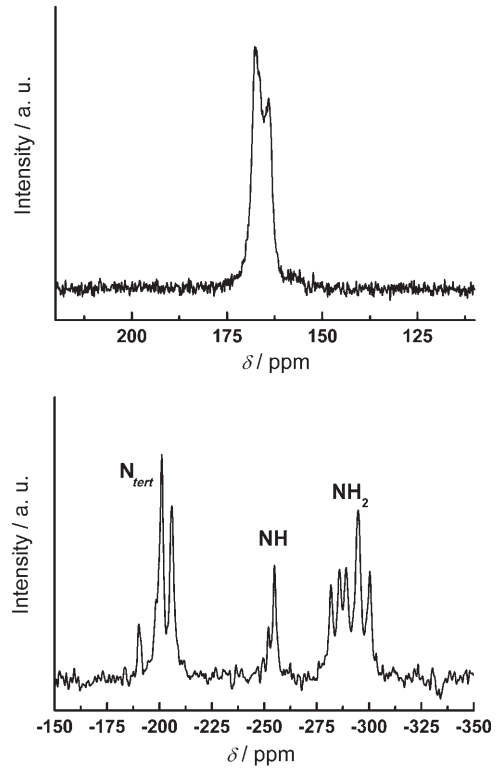

Figure 10. ^{13}C (top) and ^{15}N (bottom) CP-MAS solid-state NMR spectra of melam (recycle delay: 16 s; τ_c: 4 ms for both measurements). The spinning frequency was 10 kHz.

The ^{15}N CP-MAS NMR spectrum of melam (Figure 10, bottom) exhibits three separable tertiary nitrogen signals between $\delta = -190.0$ and -205.9 ppm, and two NH signals at $\delta = -252.0$ and -254.8 ppm, the former one being slightly less than half as intense as the latter. This finding corresponds well to the crystal structure analysis, according to which one would expect two NH groups with an intensity ratio of 2:1 (one bridging nitrogen on a special position with a site occupation factor of 0.5), which is almost exactly reproduced in the experimental spectrum. Five different NH_2 signals are visible at $\delta = -282.8$, -286.0, -288.9, -295.0, and -300.4 ppm. As for the tertiary nitrogen positions, signal overlap due to similar electronic and geometric environments must therefore be inferred, which reduces the theoretically expected numbers of independent ^{15}N signals in both cases.

The thermal behavior of melam as studied by TPXRD measurements reveals the conversion of melam into melem at 640 K without passing through the melt (see Figure S5 in the Supporting Information), and thus confirms its direct relation with this important carbon nitride precursor. The results presented above help to provide a new basis for the controversial view on melam formation from melamine.

On pyrolyzing melamine in closed or semi-closed systems as outlined above, melam is not observable as the first condensation product of the starting material, which, however, may result from its high reactivity in the respective temperature range. Similarly, the direct formation of melem from melamine without the formation of detectable intermediates lacks experimental evidence.

Van der Plaats and co-workers suggested that between 593 and 673 K melamine forms mixed crystals with its decomposition product,[36] however, without further substantiating this hypothesis. We are now in a position to confirm this view, as two intermediate phases could be isolated that are stoichiometrically built up from melamine and melem. According to NMR investigations and dissolution/extraction studies, the homogeneous phases comprise hydrogen-bonded arrays of neutral melamine and melem molecules rather than salts originating from chemical reactions of the components (acid–base reactions).

Presumably, melem is gradually formed at elevated temperatures and reintegrated into the starting material melamine, upon which a crystallographically distinct phase is formed. It may be argued that the onset of melamine sublimation greatly facilitates the condensation reaction to melem, as melamine in the gas phase may be far more reactive than the melamine residue. Note that under the reaction conditions chosen, a large amount of melamine eludes

the condensation reaction and resublimes at the cold end of the ampoule. In fact, whereas for phase I the yield amounts to 60–70%, it is only 30–35% for phase II. This finding, however, strongly suggests that the transformation from phase I into II is simply a consequence of melamine sublimation, which is thus removed from the solid. The formation of two adducts with distinct compositions may therefore be driven by the particularly beneficial arrangements of the components in the solid at the particular melamine/melem ratios, together with the possibility for melamine to be removed from the solid phase by sublimation. By this equilibrium between the solid and the gas phase, the transformation of adduct I into adduct II is feasible without major molecular rearrangements, and possibly even without further condensation of melamine into melem.

From the above statements it may be inferred that the adduct phases are only metastable at their formation temperatures, which is evidenced by the strong time dependence of their synthesis. Once the temperature sufficient for melem formation is reached, the latter is continuously produced until all melamine present in the solid is consumed. Thus, the adduct phases I and II are only intermediate stages, stable for a limited time, on the way to the thermodynamically stable product melem.

Therefore, thermal recrystallization of the adducts, which are only available as polycrystalline powders, is not feasible, as this would lead to the "extraction" of melamine from the solid. Likewise, recrystallization in solution results in the rupture of the hydrogen-bonding network and, ultimately, phase separation into the components melamine and melem.

According to our findings and as noted previously by Finkel'shtein,[27] melam is detectable to only a small extent and only under specifically tuned reaction conditions. This observation may be rationalized by invoking the formation of melam as a minor by-product instead of a true intermediate of the condensation cascade of melamine. Along these lines, a scenario may be envisaged that involves the comparatively slow, reversible formation of melam from melamine. In a parallel reaction, the latter may transform into melem via volatile species such as cyanamide or dicyandiamide, which are generated rapidly by depolymerization of melamine under increased pressure of ammonia. Melam may be transformed back into melamine at elevated temperatures, which then further reacts to melem with a significantly increased reaction rate as compared to that of melam formation. Lowering the pressure of ammonia may enhance melam formation (by slowing down the re-transformation into melamine), while depolymerization of melamine and, thus, generation of melem, is concomitantly slowed down.

However, a more straightforward rationale is the rapid consumption and further transformation of melam into melem as the condensation reaction proceeds, which is in accord with in situ X-ray studies of the thermal behavior of melam (see Figure S5 in the Supporting Information). Accordingly, melam may be viewed as a highly reactive intermediate of the thermolysis of melamine, which owing to its rapid transformation into melem is short-lived and—contrary to the adduct phases—essentially undetectable on the time scale of in situ TPXRD. The fact that melam was only observed when working in open systems may be indicative of a deceleration of its transformation kinetics with decreasing pressure as outlined above. This slow-down may again correlate with the reduced availability of ammonia in the gas phase, a species which is known to enhance melem formation.[22,48]

Melam compounds: To explore the largely unknown chemistry and structural diversity of the important CN_x precursor melam, the acid–base behavior as well as the suitability of melam as a complex ligand has been studied. Reactions in solution were carried out using melam hydrate as the starting material, solid-state reactions were conducted based on melamine and the respective salts.

The majority of the reactions carried out in acid solution yielded amorphous or poorly crystalline products that could not be fully characterized. In principle, the addition of weak acids such as acetic or formic acid to aqueous suspensions of melam hydrate only yield poorly crystalline hydrate phases, whereas strong acids form the respective melamium salts, indicating the weakly basic properties of melam by analogy to melamine and melem.[52] On prolonged refluxing of the product solutions, hydrolysis converts the melamium salts into the respective ammelinium salts.[53]

An alternative approach to melamium salts is given by reacting melamine with acid salts, preferably ammonium salts, in closed ampoules at temperatures between 623 and 723 K. This strategy is particularly intriguing as it provides access to melam on a preparative scale starting from the commercially available compound melamine. Remarkably, the tendency of melam formation from melamine is greatly enhanced in the presence of acid salts, which presumably facilitate the condensation of the triazine rings. If melamine is heated with ammonium halides, polycrystalline melam hydrohalide–ammonium halide adducts are formed, from which melam hydrate can easily be isolated on treatment with bases. This observation may rationalize the early discovery of melam by Liebig who unwittingly prepared melam via its thiocyanate or hydrochloride salt, liberating the neutral molecule by "purification" with potassium hydroxide.[1,33] We note that not only Brønstedt acids are suitable reactants but also Lewis acids such as $ZnCl_2$, $FeCl_3$, or even $CuCl_2$, which—via the respective cations—may bring the reactive triazine sites into contact by coordinating to two ring systems, thereby functioning as connectors (see Figure 13).

The crystal structures of two representative compounds of melam, which were obtained by using alternative procedures, will be highlighted in the following.

Melamium perchlorate: Melamium perchlorate (**2**) was obtained from reaction of melam hydrate with perchloric acid in aqueous solution. Relevant crystallographic data are summarized in Table 2.[51] The unit cell (space group *C*2/*c*) comprises four formula units, each consisting of a doubly pro-

tonated melam molecule, two perchlorate anions, and approximately two molecules of water of crystallization, of which one is disordered. Only one triazine ring and one perchlorate anion are contained in the asymmetric unit, therefore the cation comprises two identical triazine units and all perchlorate anions are identical.

In contrast to structures containing neutral melam molecules, the cationic melam core is planar within experimental error (Figure 11). Also, the distortion of the triazine rings is

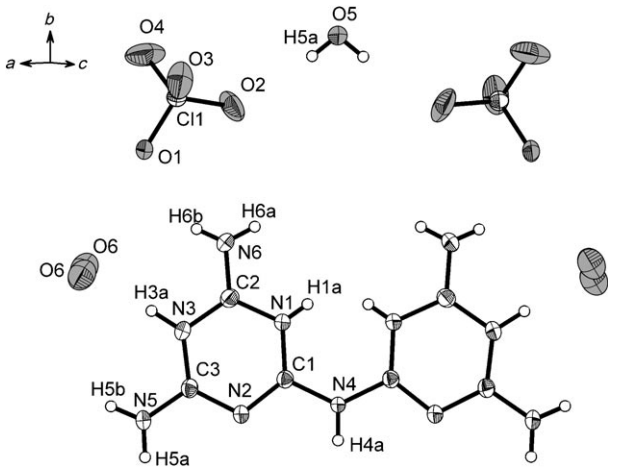

Figure 11. Representation of the molecular structure of melamium perchlorate hydrate, of which one half is contained in the asymmetric unit. The oxygen positions O6 are only half occupied, and the proton positions H1a and H3a are disordered over the melam backbone with SOFs being close to 0.5. Thermal displacement ellipsoids (except for H) are drawn at the 50% probability level.

obvious, yet less pronounced than in melam, with the average angles C-N-C and N-C-N within the rings amounting to 117° and 124°, respectively. The internal C–N distances vary between 132 and 136 pm, whereas the external C–N_{exo} bond lengths are shorter by about 2–3 pm (131/132 pm).

Notably, the two triazine rings do not possess a quinoid structure with a bridging C1–N4=C1 unit, but a C1-NH_4-C1 bridge with elongated bond lengths (138 pm). The presence of two perchlorate ions per melam molecule suggests melam to be present as a doubly protonated cation. However, four proton sites attached to the ring nitrogen atoms are found from difference Fourier synthesis, which have site occupation factors on free refinement between 0.5(1) (H3a) and 0.7(1) (H1a). Thus, disorder has to be inferred, entailing an almost equal protonation of N1 and N3 such that in total two protons are attached to the rings.

Another sign of static disorder is found at the crystal water site O6. Instead of a single oxygen a split position is found in the refinement with the centers of mass lying 119 pm apart, which is clearly too short for two adjacent water molecules. The refined site occupation factor for O6 is 0.562(9), thereby indicating an approximately equal occupation of both split positions with the sum being equal to one. It has to be noted, however, that in contrast to the situation for O5 no hydrogen positions were found around the presumed crystal water O6. The melam molecules form planar layers extending along *b*, the long molecular axes being parallel to the [10–1] direction (Figure 12). The perchlorate ions are inserted between the melam molecules, linking the latter by hydrogen contacts with donor–acceptor distances between 288 pm (N6···O1) and 301 pm (N6···O3). Remarkably, the stacking distance between adjacent planes is as small as 325 pm.

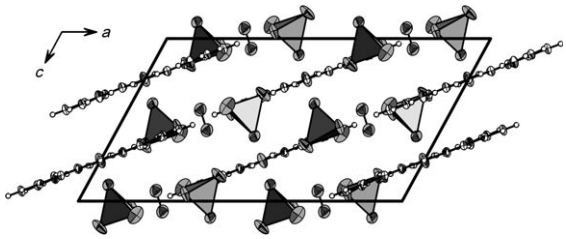

Figure 12. Unit cell of melamium perchlorate hydrate, view along [010]. Thermal displacement ellipsoids (except for H) are drawn at the 50% probability level.

Zn–melam complex $Zn[C_6N_{11}H_9]Cl_2$: The $ZnCl_2$–melam complex (**3**) was synthesized from melamine and $ZnCl_2$ in a solid-state reaction. The neutral adduct crystallizes without crystal water in the monoclinic space group $P2_1/c$ with four formula units in the unit cell. Crystallographic data for $Zn[C_6N_{11}H_9]Cl_2$ are summarized in Table 2.[51] In the molecular complex, melam functions as a neutral "ligand" coordinated to a $ZnCl_2$ molecule through the ring nitrogen atoms N2 and N5, such that the Zn1 atom is located in a distorted tetrahedral environment comprising two N and two Cl atoms (Figure 13). These results clearly disprove the assumption of Gal′perin et al. that a chloride-free Zn–melam salt containing an anionic melam core is formed upon the reaction of melamine with zinc chloride under these conditions.[46]

The steric requirements in the Lewis acid–base complex forces the melam ligand to slightly bend out of the molecular plane, thereby introducing a symmetrical (C_{2v}) distortion about the bridging nitrogen atom. Although the distortion is different from that found in pure melam, the flexibility of the N-bridged triazine core again is obvious. The triazine

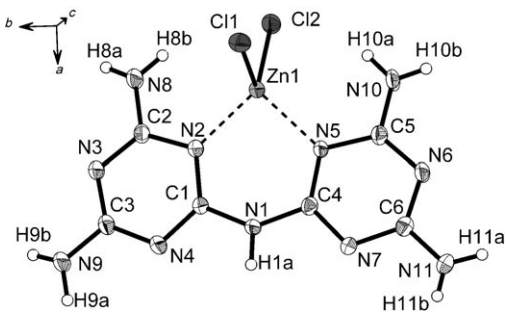

Figure 13. Asymmetric unit of the neutral zinc chloride - melam complex, in which melam functions as a bidentate ligand. Thermal displacement ellipsoids (except for H) are drawn at the 50% probability level.

rings slightly deviate from planarity, with the angles C-N-C and N-C-N systematically alternating between 114°/115° and 124°–126°, respectively. Differences in the C–N bond lengths within the rings (132–138 pm) are more pronounced than in melam and melamium perchlorate, but the variations in both rings appear to be systematic. This effect can most probably be ascribed to a drain of electron density from the ring to the Lewis acid Zn^{2+} site, which then is compensated by a rearrangement of the charge distribution according to a quinoid-type structure. The C–N_{ext} distances are on average about 2 pm (133 pm) shorter than the ring C–N bonds. The triazine rings are again bridged by a C1–N1H–C4 unit with equally elongated bond lengths (138 pm) and an angle at the imino nitrogen atom of 134°.

The complexes form undulated strands extending along [010], with neighbored melam molecules being hydrogen-bonded to each other by weak N···N contacts of 306 and 309 pm. The "layers" are spaced by approximately 362 pm and stacked irregularly such that the triazine ring planes of adjacent sheets exhibit varying offsets.

The ^{13}C solid-state CP-MAS NMR spectrum reveals three resonances, the small chemical shift differences of which indicating comparatively similar electronic environments of all ^{13}C nuclei. Nevertheless, the number of signals nicely correlates with the three different carbon positions in each ring and the symmetry of the complex. Conducting the CP measurements with different contact times as shown in Figure 14 (top) enables a differentiation between those (2 + 2) carbon atoms adjacent to amino groups ($\delta = 163.4/165.7$ ppm), which exhibit faster magnetization transfers from the proton bath, and those two which are neighbored to the bridging NH group ($\delta = 161.4$ ppm) and exhibit higher intensity at longer contact times (spectrum a; Figure 14 top).

In the ^{15}N CP-MAS NMR spectrum (Figure 14 (bottom), top spectrum) six signal groups are found, of which the signals at $\delta = -193.8$ and -207 ppm are located in the chemical shift range characteristic of the tertiary nitrogen atoms of triazine rings. The signal at $\delta = -54.0$ ppm exhibits a chemical shift typical of NH groups, whereas the signals at $\delta = -280.7$ and -291.6 ppm lie in the NH_2 region. The signal at $\delta = -238.1$ ppm is located intermediate between the N_{tert} and NH region and can—apart from chemical considerations based on the crystal structure—not be assigned unambiguously without further data. Thus, a CPPI experiment has been carried out with an inversion time typical for NH signals to pass zero intensity (160 μs).[22] As shown in Figure 14 (bottom), bottom spectrum, the magnetization of the NH signal at $\delta = -254$ ppm is zero, whereas according to the expectations that of the NH_2 groups is negative. The signal at $\delta = -238$ ppm clearly has hardly lost intensity and can therefore be assigned to a tertiary nitrogen resonance.

The above results suggest that the coordination of melam at two ring nitrogen sites to the Zn cation leads to a high-field shift for the ^{15}N nuclei (shielding). The remaining two signals can then be attributed to ring nitrogen sites not involved in the Zn coordination. Two of the four amino groups exhibit almost identical chemical shifts each, so that the observation of two NH_2 signals can be rationalized.

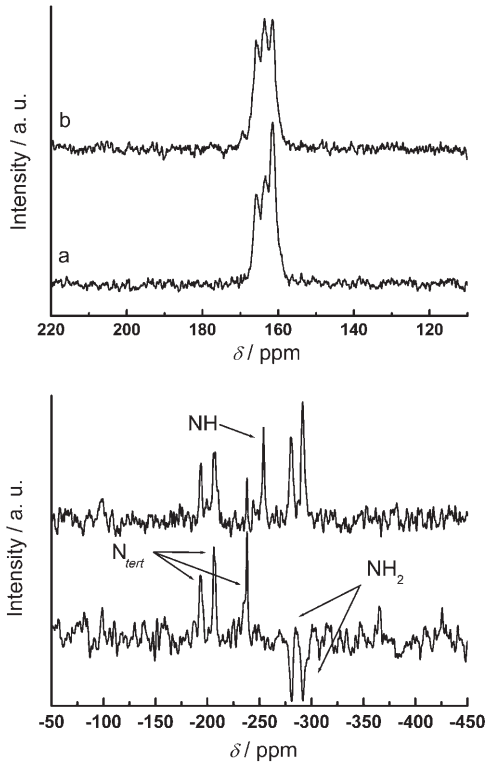

Figure 14. CP-MAS solid-state NMR spectra of the melam–$ZnCl_2$ complex. Top: ^{13}C spectra recorded with two different contact times to identify the proton environment of the different carbon sites (top curve: 2 ms, bottom curve: 10 ms; recycle delay: 60 s). Bottom: ^{15}N CP (top curve, spinning frequency 10 kHz) and CPPI spectra (bottom curve, spinning frequency 5.5 kHz); the signal assignments are indicated (recycle delay: 60 s; τ_c: 4 ms; inversion time τ_i: 160 μs).

Conclusion

In summary, we have comprehensively delineated the thermal condensation of melamine, which was shown to yield two crystallographically distinct phases composed of neutral melamine and melem molecules prior to melem formation, if the reaction is conducted under the pressure of ammonia. At ambient pressure small amounts of melam single crystals can be isolated, which may be considered either as a *side product* or, more likely, as a short-lived, reactive intermediate which is rapidly transformed into melem by means of further ammonia elimination. We hypothesize that owing to the initial lack of analytical data apart from elemental analysis, the 2:1 co-crystallizate of melamine and melem may have easily been mistaken for melam. Nevertheless, melam can be produced on a preparative scale by reacting melamine with acid salts and treating the resulting melamium salts with aqueous bases, upon which melam hydrates are formed. Melam crystallizes in a "ditriazinylamine"-type structure, in which the two triazine rings are twisted with respect to each other. Protonated melam cations, which are

unstable in neutral aqueous solution owing to their acid properties, adopt an essentially planar structure, whereas the melam backbone in the neutral $ZnCl_2$–melam complex is symmetrically bent, thereby demonstrating the significant steric flexibility of this potential "bidentate" complex ligand and precursor for graphitic carbon nitride.

Experimental Section

Synthesis

Adducts I and II: The adduct phases I and II (see text) were synthesized by heating melamine (200 mg, 1.59×10^{-3} mol, $\geq$99%, Fluka) in a sealed Duran ampoule (length 120 mm, $\varnothing_{ext}$ 16 mm, $\varnothing_{int}$ 13 mm) placed in a vertical tube furnace at 663 K with a heating rate of 1 K min^{-1}. The tempering time for adduct I was 2.5 h, for adduct II 14 h were appropriate (for lower temperatures down to 630 K, the tempering time had to be readjusted, that is prolonged depending on the exact temperature). Data for adduct I: ^{1}H NMR (400 MHz, [D$_6$]DMSO, TMS): $\delta=7.3$ (s, 6H; NH_2), 6.0 (s, 12H; NH_2) ppm; $^{13}C\{^1H\}$ NMR (400 MHz, [D$_6$]DMSO, TMS): $\delta=167.0$, 165.1, 155.3 ppm; MS (70 eV, DEI$^+$): *m/z* (%): 126.1 (100) $[C_3N_6H_6]^+$, 218.1 (100) $[C_6N_{10}H_6]^+$ (relative intensities refer to successive scans); data for adduct II: ^{1}H NMR (400 MHz, [D$_6$]DMSO): $\delta=$ 7.3 (s, 12H; NH_2), 6.0 (s, 6H; NH_2) ppm; $^{13}C\{^1H\}$ NMR (400 MHz, [D$_6$]DMSO): $\delta=167.5$, 165.6, 155.8 ppm; MS (70 eV, DEI$^+$): *m/z* (%): 126.1 (70) $[C_3N_6H_6]^+$, 218.1 (100) $[C_6N_{10}H_6]^+$. For further analytical data see text.

Melam: A porcelain crucible of about 2 cm height and 1 cm diameter was loaded with 2–10 g melamine, loosely covered with a lid and placed in a muffle furnace. After heating at 613–633 K for approximately two days, tiny colorless crystals had formed on the surface of the grayish bulk material. Melam used for the solid-state NMR investigations and thermal analysis was obtained from melam hydrate "$C_6N_{11}H_9\cdot2H_2O$", which was placed in a muffle furnace and dehydrated at temperatures between 423 and 572 K for 1–2 days. The product obtained was identified as melam by IR spectroscopy and X-ray powder diffraction (low crystallinity). ^{1}H NMR (270 MHz, [D$_6$]DMSO, TMS): $\delta=9.2$ (s, 1H; NH), 6.6 (s, 8H; NH_2) ppm; $^{13}C\{^1H\}$ NMR (270 MHz, [D$_6$]DMSO, TMS): $\delta=167.6$, 164.6 ppm; IR (KBr): $\tilde{\nu}=3483.8$ (vw), 3456.5 (vw), 3300.2 (w), 3165.4 (w), 1687 (vw), 1639.5 (m), 1610.0 (m), 1583.8 (s), 1545.8 (s), 1513.1 (s), 1450.8 (s), 1414.7 (vs), 1338.4 (vs), 1249.8 (s), 1174.9 (w), 1069.9 (vw), 1021.1 (vw), 972.2 (vw), 806.2 (vs), 782.1 (w), 748.0 (vw), 682.6 (m), 632.2 (s) cm^{-1}; MS (2.5 kV, ESI$^+$): *m/z* (%): 236.11 (69) $[M+H]^+$; elemental analysis calcd (%) for $C_6N_{11}H_9$ (235.2): C 30.63, N 65.53, H 3.83; found: C 30.67, N 64.25, H 3.60. For further analytical data see text.

Melam hydrate: Melam hydrate was obtained from a melam–NH_4Cl adduct of approximate composition $[C_6N_{11}H_{10}]Cl\cdot0.5\,NH_4Cl$. The adduct was synthesized by heating melamine (364.4 mg, 2.89×10^{-3} mol, $\geq$99%, Fluka) and NH_4Cl (91.9 mg, 1.72×10^{-3} mol, $\geq$99.5%, Fluka) at 723 K for 12 h (heating rate 1 K min^{-1}) in a glass ampoule with ground neck (length 200 mm, $\varnothing_{ext}$ 25 mm, $\varnothing_{int}$ 22 mm).[48] The obtained melam–NH_4Cl adduct (550 mg, 1.84×10^{-3} mol) was stirred in aqueous NH_3 (60 mL, 25% (p. a.), Merck) for 1 h to remove the ammonium chloride and subsequently air-dried. According to elemental analysis and vibrational spectroscopy, products with the approximate composition "$C_6N_{11}H_9\times2H_2O$" were obtained, though slightly varying water content was observed in different samples. IR (KBr): $\tilde{\nu}=3463.0$ (m), 3336.9 (m), 3184.0 (m), 1623.0 (s, b), 1548.8 (s), 1525.4 (s), 1427.9 (s), 1350.8 (s), 1262.4 (m), 1183.6 (w), 1087.1 (vw), 1031.9 (w), 810.1 (m), 790.1 (vw), 740.7 (vw), 623.1 (vw), 614.5 (w), 591.9 (vw), 507.5 (vw) cm^{-1}; MS (2.5 kV, ESI$^+$): *m/z* (%): 236.11 (67) $[(M-2H_2O)+H]^+$; elemental analysis calcd (%) for $C_6N_{11}H_9\cdot2H_2O$ (271.2): C 26.57, N 56.83, H 4.80; found: C 26.36, N 55.44, H 4.85.

Melamium perchlorate hydrate: Melam hydrate (200 mg, 7.38×10^{-3} mol) was suspended in water (110 mL) and heated under reflux. $HClO_4$ (3 mL, 60% (p. a.), Merck) was added dropwise until a clear solution was obtained. The solution was refluxed for another five minutes, then cooled down and stored in the refrigerator until colorless needles began to crystallize. IR (KBr): $\tilde{\nu}=3608.2$ (w), 3536.1 (w), 3419.6 (m), 3347.9 (m), 3256.9 (m), 2868.7 (w), 2748.7 (w), 1686.7 (m), 1639.8 (s), 1560.2 (m), 1525.5 (w), 1478.5 (w), 1444.9 (m), 1394.7 (m), 1328.5 (m), 1262.3 (m), 1088.6 (s), 1060.4 (s), 1018.1 (m), 993.1 (w), 931.5 (vw), 876.5 (vw), 800.7 (vw), 787.0 (m), 740.6 (vw), 627.3 (m), 583.5 (w), 512.2 (w) cm^{-1}. MS (70 eV, DEI$^+$): *m/z* (%): 18 (100) $[H_2O]$, 126.1 (68) $[C_3N_6H_6]^+$, 235.1 (70) $[C_6N_{11}H_9]^+$; (6 kV, FAB$^+$): *m/z* (%): 236.2 (5) $[C_6N_{11}H_{10}]^+$; elemental analysis calcd (%) for $[C_6N_{11}H_{11}][ClO_4]_2\times2H_2O$ (472.2): C 15.26, N 32.63, H 3.18; found: C 16.08, N 34.24, H 3.22.

Melam–zinc dichloride: Melamine (200 mg, 1.59×10^{-3} mol) was intimately mixed with $ZnCl_2$ (108 mg, 7.95×10^{-3} mol) and quickly transferred into a Duran ampoule (length 120 mm, $\varnothing_{ext}$ 16 mm, $\varnothing_{int}$ 13 mm), which was sealed under dry argon. The ampoule was placed in a vertical tube furnace and heated at 703 K for 12 h (heating rate 1 K min^{-1}). IR (KBr): $\tilde{\nu}=3454.8$ (s), 3447.2 (s), 3429.3 (s), 3349.6 (s), 3179.1 (m), 1671.5 (s), 1645.7 (s), 1620.5 (s), 1568.3 (m), 1548.1 (s), 1474.0 (m), 1418.1 (s), 1358.1 (s), 1302.8 (m), 1155.3 (w), 1109.2 (w), 1089.3 (vw), 1016.0 (w), 799.8 (s), 769.1 (w), 738.8 (vw), 722.0 (w), 694.8 (w), 629.0 (m), 601.7 (w), 570.5 (w), 518.6 (vw), 460.5 (w) cm^{-1}. MS (DCI$^+$): *m/z* (%): 127.2 (26) $[(C_3N_6H_6)+H]^+$; (70 eV, DEI$^+$): *m/z* (%): 36.0 (100) [HCl], 126.1 (24) $[C_3N_6H_6]^+$, 235.1 (0.1) $[C_6N_{11}H_9]^+$; elemental analysis calcd (%) for $Zn[C_6N_{11}H_9]Cl_2$ (371.5): C 19.39, N 41.57, H 2.42, Cl 19.09, Zn 17.60; found: C 18.82, N 40.52, H 2.50, Cl 19.98, Zn 18.50.

General methods: ^{1}H and ^{13}C NMR spectra were recorded as [D$_6$]DMSO solutions on a JEOL Eclipse EX-400 instrument, the chemical shifts being referenced with respect to TMS.

Mass spectra were obtained by using a Jeol MStation JMS-700 gas inlet system. The substance was dissolved in a 3-nitrobenzyl alcohol matrix (FAB$^+$) on a target and ionized by bombardment with accelerated (6 kV) Xe atoms. Direct insertion DEI$^+$ (70 eV) mass spectra were obtained by using a Jeol MStation JMS-700 gas inlet system. Electrospray Ionisation (ESI) measurements were conducted on a Finnigan MAT 95Q and a Finnigan MAT 90 mass spectrometer using an API-Interface II with an ESI probe head and a capillary voltage of 2.5 kV.

Elemental analyses were performed by using a commercial C, H, N elemental analyzer system Vario EL (Elementar Analysensysteme GmbH).

X-ray diffraction: Single crystals of melam (**1**) and the zinc chloride–melam complex (**3**) were measured on an Enraf–Nonius Kappa CCD diffractometer equipped with a rotating anode, and X-ray diffraction data of melamium perchlorate hydrate (**2**) were recorded on a STOE IPDS diffractometer using graphite-monochromated $Mo_{K\alpha}$ radiation ($\lambda=$ 71.073 pm). The crystal structures were solved by direct methods using the program SHELXS-97[54] and refined on F^2 by applying the full-matrix least-squares method implemented in SHELXL-97.[55] For the $ZnCl_2$–melam complex a multi-scan absorption correction was carried out that is routinely included in the software packages DENZO and SCALEPACK.[56] The positions of all hydrogen atoms were determined from difference Fourier syntheses and refined without constraints; all non-hydrogen atoms were refined anisotropically. Details of the crystal structure determinations and refinements are summarized in Table 2.[51]

High-temperature in situ X-ray diffraction was carried out on a STOE Stadi P powder diffractometer (Ge(111)-monochromated Mo-$K_{\alpha1}$ radiation, $\lambda=70.093$ pm) with an integrated furnace using unsealed quartz capillaries ($\varnothing$ 0.5 mm) as sample containers. Data were collected in a 2θ range of approximately 3–17° with an average scan collection time of 30 minutes. The samples were heated from 298 K to temperatures around 923 K in steps of 10 K min^{-1}, using a heating rate of 20 K min^{-1} between the scans.

Solid-state NMR spectroscopy: ^{15}N and ^{13}C CP-MAS solid-state NMR spectra were recorded by using natural abundance samples at ambient temperature on a conventional impulse spectrometer DSX 500 Avance (Bruker) operating at 500 MHz. The samples were contained in 4-mm ZrO_2 rotors, which were mounted in a standard double-resonance MAS probe head (Bruker). The ^{15}N signals were referenced with respect to nitromethane, the ^{13}C signals to TMS. A ramped cross-polarization sequence was employed to excite the ^{15}N/^{13}C nuclei via the proton bath; the power of the ^{1}H radiation was linearly varied about 50%. The data

collection of all experiments was performed by applying broadband proton decoupling using a TPPM sequence.[57] CPPI experiments (cross-polarization combined with polarization inversion) were performed to probe the number of hydrogen atoms directly attached to the nitrogen nuclei.[22,49] Typically, the contact times τ_c for both CP and CPPI experiments were 2–10 ms, while the inversion time τ_i in the CPPI experiments was set to 100–160 μs such that the polarization of NH groups was close to zero.[22] The recycle delays were estimated from ^{1}H $T1$ measurements. Sample spinning frequencies of 10 kHz and 5 or 5.5 kHz for CP and CPPI experiments, respectively, were employed.

IR spectroscopy: FTIR measurements were carried out on a Bruker IFS 66v/S spectrometer. Spectra of the samples were recorded as KBr pellets (1 mg sample, 500 mg KBr, hand press with press capacity 10 kN) in an evacuated cell equipped with a DLATGS detector at ambient conditions between 400 and 4000 cm^{-1}. IR spectra of the neat solids (650–4000 cm^{-1}) were recorded in reflection geometry using a Perkin Elmer Spectrum BXII FT-IR spectrometer equipped with a DuraSampl*IR* II diamond ATR device (Smith Detection).

Thermal analysis: Thermoanalytical measurements between room temperature and 873 K were conducted on a Mettler DSC 25 with a heating rate of 1 K min^{-1}. The cold-welded, only moderately pressure-resistant aluminum crucible used as sample container was placed in the calorimeter under an atmosphere of dry nitrogen.

Acknowledgements

We thank W. Wünschheim for conducting the DSC measurements and Dr. P. Mayer, Dr. O. Oeckler, and T. Miller for single-crystal X-ray data collection. The authors gratefully acknowledge financial support that was granted from the Deutsche Forschungsgemeinschaft (DFG) (project SCHN 377/12–1), Fonds der Chemischen Industrie, the BMBF and the Studienstiftung des Deutschen Volkes (scholarships for B. V. Lotsch).

[1] J. von Liebig, *Ann. Pharm.* **1834**, *10*, 1.
[2] E. Kroke, M. Schwarz, *Coord. Chem. Rev.* **2004**, *248*, 493.
[3] S. Matsumoto, E. Q. Xie, F. Izumi, *Diamond Relat. Mater.* **1999**, *8*, 1175.
[4] S. Muhl, J. M. Mendez, *Diamond Relat. Mater.* **1999**, *8*, 1809.
[5] C.-M. Sung, M. Sung, *Mater. Chem. Phys.* **1996**, *43*, 1.
[6] M. L. Cohen, *Phys. Rev. B* **1985**, *32*, 7988.
[7] M. L. Cohen, *Science* **1993**, *261*, 307.
[8] A. Y. Liu, M. L. Cohen, *Science* **1989**, *245*, 841.
[9] A. Y. Liu, M. L. Cohen, *Phys. Rev. B* **1990**, *41*, 10727.
[10] C. Niu, Y. Z. Lu, C. M. Lieber, *Science* **1993**, *261*, 334.
[11] D. M. Teter, R. J. Hemley, *Science* **1996**, *271*, 53.
[12] E. Kroke, M. Schwarz, E. Horath-Bordon, P. Kroll, B. Noll, A. D. Norman, *New J. Chem.* **2002**, *26*, 508.
[13] I. Alves, G. Demazeau, B. Tanguy, F. Weill, *Solid State Commun.* **1999**, *109*, 697.
[14] D. R. Miller, D. C. Swenson, E. G. Gillan, *J. Am. Chem. Soc.* **2004**, *126*, 5372.
[15] D. T. Vodak, K. Kim, L. Iordanidis, P. G. Rasmussen, A. J. Matzger, O. M. Yaghi, *Chem. Eur. J.* **2003**, *9*, 4197.
[16] T. Komatsu, *J. Mater. Chem.* **2001**, *11*, 799.
[17] T. Komatsu, T. Nakamura, *J. Mater. Chem.* **2001**, *11*, 474.
[18] J. Kouvetakis, A. Bandari, M. Todd, B. Wilkens, *Chem. Mater.* **1994**, *6*, 811.
[19] Z. H. Zhang, K. Leinenweber, M. Bauer, L. A. J. Garvie, P. F. McMillan, G. H. Wolf, *J. Am. Chem. Soc.* **2001**, *123*, 7788.
[20] B. V. Lotsch, W. Schnick, *Chem. Mater.* **2005**, *17*, 3976.
[21] B. V. Lotsch, W. Schnick, *Chem. Mater.* **2006**, *18*, 1891.
[22] B. Jürgens, E. Irran, J. Senker, P. Kroll, H. Müller, W. Schnick, *J. Am. Chem. Soc.* **2003**, *125*, 10288.
[23] A. Sattler, W. Schnick, *Z. Anorg. Allg. Chem.* **2006**, *632*, 238.
[24] E. C. Franklin, *J. Am. Chem. Soc.* **1922**, *44*, 486.
[25] C. E. Redemann, . H. J. Lucas, *J. Am. Chem. Soc.* **1940**, *62*, 842.
[26] H. May, *J. Appl. Chem.* **1959**, *9*, 340.
[27] A. I. Finkel'shtein, *Russ. J. Gen. Chem.* **1961**, *31*, 1046.
[28] N. K. Gavrilova, V. A. Gal′perin, A. I. Finkel'shtein, A. G. Koryakin, *Zh. Org. Khim.* **1977**, *13*, 669.
[29] L. Costa, G. Camino, *J. Therm. Anal. Calorim.* **1988**, *34*, 423.
[30] C. Voelckel, *Ann. Chim. Phys.* **1844**, *62*, 90.
[31] W. L. Burdick, *J. Am. Chem. Soc.* **1925**, *47*, 1485.
[32] E. W. Hughes, *J. Am. Chem. Soc.* **1941**, *63*, 1737.
[33] P. Klason, *J. Prakt. Chem.* **1886**, *33*, 285.
[34] B. Bann, S. A. Miller, *Chem. Rev.* **1958**, *58*, 131.
[35] G. B. Seifer, *Russ. J. Coord. Chem.* **2002**, *28*, 301.
[36] G. van der Plaats, H. Soons, R. Snellings, *Proc. Eur. Symp. Therm. Anal. 2nd* **1981**, 215.
[37] A. I. Finkel'shtein, *Opt. Spectra* **1959**, *6*, 33.
[38] M. Takimoto, *Kogyo Kagaku Zasshi* **1961**, *64*, 1452.
[39] M. Takimoto, *Kogyo Kagaku Zasshi* **1964**, *85*, 168.
[40] N. V. Spiridonova, A. I. Finkel'shtein, *Khim. Geterotsikl. Soedin.* **1966**, *1*, 126.
[41] W. J. Schnabel, R. Rätz, E. Kober, *J. Org. Chem.* **1962**, *27*, 2514.
[42] S. Tragl, K. Gibson, H.-J. Meyer, *Z. Anorg. Allg. Chem.* **2004**, *630*, 2373.
[43] T. Tojima, R. Saito (Mitsubishi Engineering-Plastic Corp.), JP-2004217687 A2, **2004** [*Chem. Abstr.* **2004**, *141*, 157944].
[44] E. Schlosser, B. Nass, W. Wanzke, EP-1386942 A1, **2004** [*Chem. Abstr.* **2004**, *140*, 147040].
[45] P. Flippo, J. Tijssen, C. K. Sham, A. E. H. De Keijzer, R. J. M. Hulskotte, US-2001008913 A1, **2001** [*Chem. Abstr.* **2004**, *135*, 93449].
[46] V. A. Gal′perin, A. I. Finkel'shtein, N. K. Gavrilova, *Zh. Org. Khim.* **1971**, *7*, 2431.
[47] L. Costa, G. Camino, G. Martinasso, *Polym. Prepr. Am. Chem. Soc. Div. Polym. Chem.* **1989**, *30*, 531.
[48] B. Jürgens, Ph. D. thesis, University of Munich (Germany), Shaker Verlag: Aachen, **2004**.
[49] C. Gervais, F. Babonneau, J. Maquet, C. Bonhomme, D. Massiot, E. Framery, M. Vaultier, *Magn. Reson. Chem.* **1998**, *36*, 407.
[50] The slight low-field shift observed for the ^{1}H and ^{13}C melamine signals is presumably due to differences in the instrument calibration or concentration effects, since a 2:1 mixture of melamine and melem yields an essentially identical spectrum to that of phase I (see Supporting Information).
[51] CCDC-618430 (**1**), CCDC-618432 (**2**), and CCDC-618431 (**3**) contain the supplementary crystallographic data for this paper. These data can be obtained free of charge from the Cambridge Crystallographic Data Centre via www.ccdc.cam.ac.uk/data request/cif.
[52] A. Sattler, Diploma Thesis, University of Munich (Germany), **2005**.
[53] B. V. Lotsch, W. Schnick, *Z. Anorg. Allg. Chem.* **2006**, *632*, 1457.
[54] G. M. Sheldrick, SHELXS97, Program for the Solution of Crystal Structures, University of Göttingen, Göttingen (Germany), **1997**.
[55] G. M. Sheldrick, SHELXL97, Program for the Refinement of Crystal Structures, University of Göttingen, Göttingen (Germany), **1997**.
[56] Z. Otwinowsky, W. Minor, *Methods Enzymol.* **1997**, *276*, 307.
[57] A. E. Bennett, C. Rienstra, M. Auger, K. V. Lakshmi, R. G. Griffin, *J. Chem. Phys.* **1995**, *103*, 6951.

Received: September 7, 2006
Revised: February 12, 2007
Published online: April 5, 2007

